

Mechanical Design of a Cartesian Manipulator for Warehouse Pick and Place

M. McTaggart^{1,2}, R. Smith^{1,2}, J. Erskine^{1,2}, R. Grinover^{1,2}, A. Gurman^{1,2}, T. Hunn^{1,2}, N. Kelly-Boxall^{1,2}, D. Lee^{1,2}, A. Milan^{1,3}, D. Morrison^{1,2}, T. Pham^{1,3}, G. Rallos^{1,2}, A. Razjigaev^{1,2}, T. Rowntree^{1,3}, K. Vijay^{1,3}, S. Wade-McCue^{1,2}, A.W. Tow^{1,2}, Z. Zhuang^{1,4}, J. Leitner^{1,2}, I. Reid^{1,3}, P. Corke^{1,2}, and C. Lehnert²

Abstract—Robotic manipulation and grasping in cluttered and unstructured environments is a current challenge for robotics. Enabling robots to operate in these challenging environments have direct applications from automating warehouses to harvesting fruit in agriculture. One of the main challenges associated with these difficult robotic manipulation tasks is the motion planning and control problem for multi-DoF (Degree of Freedom) manipulators. This paper presents the design and performance evaluation of a low cost Cartesian manipulator, *Cartman* who took first place in the Amazon Robotics Challenge 2017. It can perform pick and place tasks of household items in a cluttered environment. The robot is capable of linear speeds of 1 m/s and angular speeds of 1.5 rad/s, capable of sub-millimetre static accuracy and safe payload capacity of 2kg. *Cartman* can be produced for under 10 000 AUD. The complete design is open sourced and can be found at <http://juxi.net/projects/AmazonRoboticsChallenge/>.

I. INTRODUCTION

Enabling robots to pick and place items within cluttered and challenging environments has direct application to industries such as e-commerce, logistics and even agriculture. One of the main challenges associated with these difficult robotic manipulation tasks is the motion planning and control for multi-DoF (Degree of Freedom) manipulators [1]. This can be difficult in scenarios where the environment is cluttered, dynamic and unstructured [2] requiring large amounts of computational time to find a collision-free path in the configuration space of the manipulator. In this paper we argue that designing a manipulator which reduces the complexities of solving the motion planning problem can lead to robust and reliable solutions for real-world deployment.

Robotics competitions are a great driver for developing robotic solutions that are reliable in real world scenarios. Amazon hold an annual competition in which they invite 16 teams from around the world to help solve their warehouse automation problem. The competition requires teams to design a robotic picking solution that can autonomously pick and place a variety of household items. This manipulator design forms part of our winning entry to the Amazon Robotics Challenge 2017 [3].

This research was supported by the Australian Research Council Centre of Excellence for Robotic Vision (ACRV) (project number CE140100016). The participation at the ARC was supported by Amazon Robotics LLC. Contact: matthew.mctaggart@roboticvision.org

¹Authors are with the Australian Centre for Robotic Vision (ACRV).

²Authors are with the Queensland University of Technology (QUT).

³Authors are with the University of Adelaide.

⁴ZZ is with the Australian National University (ANU).

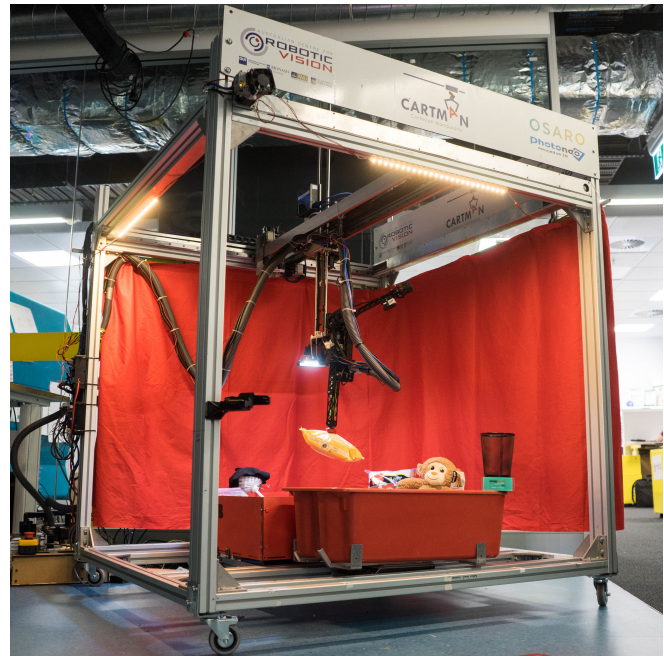


Fig. 1. *Cartman*, a cartesian manipulator for pick and place applications. *Cartman* is composed of six degrees of freedom; three prismatic joints which form the X-, Y- and Z-axes and three revolute joints and a multi-modal end effector for grasping a large range of items.

The Amazon Robotics Challenge involves two tasks, stowing and picking. Stowing is the task of picking items from a cluttered tote and placing them into a storage unit [4], emulating the task of storing items received from external suppliers. Picking is the task of taking items from the storage unit and placing them into boxes that are to be delivered to your door. Depending on the storage system, the task essentially requires large vertical motion and horizontal planar motion.

Based on previous experiences, the most common type of manipulators used for this challenge are fully articulated, a UR-5 and Baxter [5]. The main advantage of using an articulated manipulator is the ratio of mechanical footprint to workspace. However, using a fully articulated manipulator comes with the challenges such as singularities [1] in the inverse kinematics which can cause the motion plan to fail or result in unwanted large joint velocities [6]. A bigger issue for robotic pick and place tasks is that the tip position is

defined by the item to be grasped which give fewer options for the configuration of the arm to achieve a successful grasp. Collisions are likely in this situation. The advantage with Cartesian robots is that they have the same shape irrespective of tool position.

Cartesian manipulators are comprised of three orthogonal linear actuators. If there is no requirement for a small mechanical footprint or the structure of the environment is not complex, such as a mobile manipulation task, then Cartesian manipulators are well suited. Planning times are faster due to simpler inverse kinematics because the configuration space is the task space.

In this paper we propose a cost-effective design of a Cartesian robot (seen in Fig. 1) for pick and place tasks along with extensive performance measures. In particular, the contributions of this paper include:

- The cost-effective design of a 6 DoF Cartesian manipulator.
- Novel differential belt drive system to assist with single motors driving all distal motors.
- Extensive performance analysis verifying the design for use in pick and place tasks

It features six degrees of freedom; three prismatic joints which form the X-, Y- and Z-axes and three revolute joints which form the wrist allowing the end effector to have a roll, pitch and yaw motion. The complete design is open sourced and is available online at <http://juxi.net/projects/AmazonRoboticsChallenge/>. A detailed system overview or our system of the Amazon Robotics Challenge task can be found in [3].

This paper presents a brief comparison between Cartesian and articulated manipulators (Section II), design (Section III) and performance evaluation (Section IV) and a discussion of our low-cost Cartesian manipulator. The robot arm has the ability to be used in other scenarios in which a large planar workspace is available, such as fruit harvesting in a greenhouse [7] or factory pick and place tasks.

II. CARTESIAN VS ARTICULATED

Articulated manipulators are common for many different applications due to their versatility and large workspace with respect to their mechanical footprint. The drawbacks are that they can have singularities and discontinuity in trajectory for certain end effector configurations [8] [6]. There are ways of reducing the effect of singularities on motion planning but not eliminating them as shown in the works of [9] and [10]. Using a Cartesian manipulator with a wrist joint to work in a cartesian work space eliminates almost all singularities and reduces discontinuities. A comparison between Cartesian and other articulated robots can be seen in Fig. 2. These discontinuities only affect the end-effectors if they try to rotate through them. Since Cartesian works in a primarily vertical direction without rotating the wrist joint, these discontinuities do not affect regular operation of the robot. A disadvantage with a cartesian manipulator is the requirement for a larger mechanical footprint in ratio to the overall workspace of the manipulator. This is due to the fact that the linear motion

requires some form of support, usually a rail, along the entire length of the axis.

III. DESIGN

III-A Overview

The entire manipulator system is mounted on an aluminium stand shown in Fig. 4. It has three linear axes and a wrist joint which consists of a roll, pitch and yaw axes. Also featured in Fig. 4 is the gripper [11].

III-B Specifications

When designing the manipulator for the Amazon Robotics Challenge task we set out the following specifications:

- A reachable workspace of $1.2\text{m} \times 1.2\text{m} \times 1.0\text{m}$
- A top linear velocity of 1m/s under load along the three linear axes (X, Y and Z).
- A top angular velocity of 1rad/s under load in the angular axes (roll, pitch and yaw).
- Have a load capacity of 2kg .
- Six DoF at the end-effector, given by three linear axes forming the Cartesian gantry and a three-axis wrist.
- Be able to be easily deconstructed/reconstructed for transportation overseas to the Amazon Robotics Challenge event location.

III-C Mechanical Design

Frame: The frame design is constructed out of laser cut and folded 1.2mm sheet aluminium. This was used to keep weight down for transport. The sheet aluminium formed the main outer frame for the system and housed the X-axis belt system and transmission rod. The manipulator frame is mounted on an aluminium stand as seen in Fig. 4.

Motors: Linear motion is performed using Technic's ClearPath SD-SK-2311S motors. They are a closed-loop brushless motor system designed to be a drop in replacement for stepper motors. By using a stepper-like motor, eliminates the need for external encoders, and makes controlling the linear axes quite simple and similar to how a 3D printer is controlled. They were chosen due their high performance and ease of use.

For the roll, pitch and yaw axes, three Dynamixel Pro L54-50-500 are used. These motors provide the necessary operating torque to hold a 2kg on the end effector whilst under acceleration.

Power Transmission: To actuate the prismatic joints, a belt and pulley system was used. A single motor drives the X-axis. In order to eliminate a cantilever effect on the X-axis, a transmission rod is used to transmit power from one member to another. One common design that has been observed in a lot of simple manipulator designs, is each axis motor needs to carry the weight of all distal motors as well as the payload. As a result, more powerful motors are needed which then increases weight as well as cost. To solve this problem a differential belt system was designed. Rather than using a single motor to drive a single axis, two

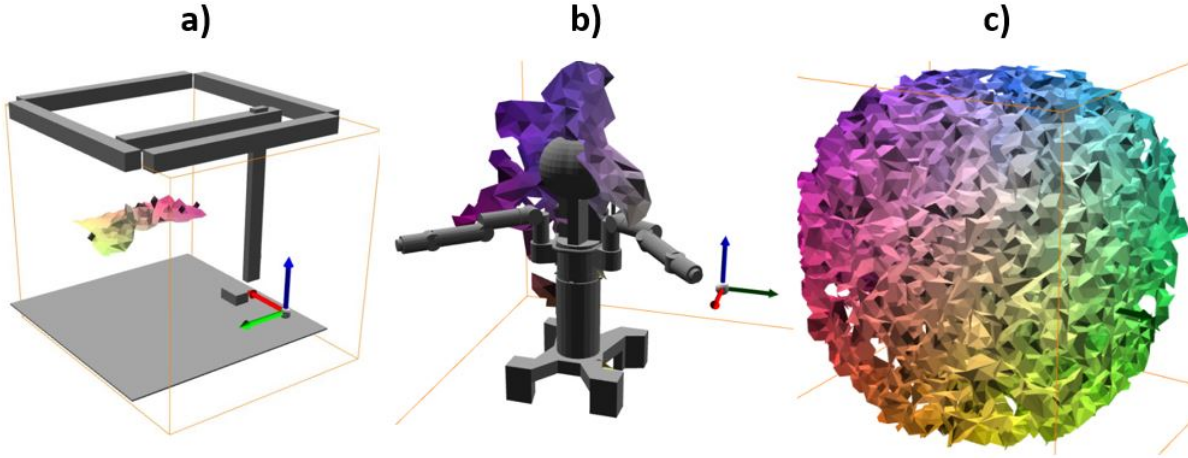


Fig. 2. Comparison of discontinuity maps between Cartman, a Baxter and UR-5. (a) Map of Cartman's sucker end-effector, (b) Map of Baxter's left gripper, (c) Map of the UR-5 end-effector. If the end-effector passes through these boundaries, joint velocities can accelerate to infinity. Cartman's design limits these discontinuity boundaries, making planning simpler and safer.

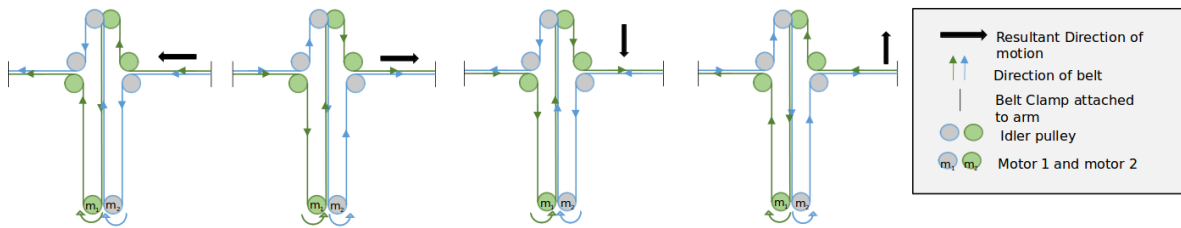


Fig. 3. Differential belt system implemented for Y- and Z-axes. The resulting motion of the arm is the sum of the individual belt vectors. In this example, the four middle idler pulleys are able to move in the vertical plane. Diagonal motion is obtainable by combination of two of the examples.

motors work in tandem to drive two axes. The system can be seen in Fig. 3.

Rails and Bearings: The linear rails used for the X- and Y-axes are the TBR20 and TBR15 respectively. These are a precision type profile rail which offer a higher precision compared to other linear type rails. Smaller rails were used in the Y-axis to reduce weight on the system. The Y-axis consists of two 10mm round rails. Although 10mm rails are relatively small for the application, they offer a light-weight. The downside to using 10mm rails, however, is that when the Z-axis is extended it creates a pendulum and induces oscillations at the end effector due to deflection. This was a trade-off that was considered during the design process. Although deflection and oscillations are present, steady state accuracy is still achieved with ease once settled. Additionally, the oscillations can be minimised by raising the Z-axis when performing large transnational movements.

III-D Electrical Design

A single microcontroller is used to control all six axes. The microcontroller that was chosen was the Teensy 3.6 as

many libraries exist and has a suitable processor capable of over 180MHz operation. The breakout board needed to include a logic shifter circuits for each of the ClearPath motor pins as the input and output threshold for this microcontroller is only 3.3V and the ClearPath motors needed minimum 5V pulse to operate. In order to interface with the Dynamixel Pro motors, an RS485 module was used so that the Teensy could communicate using the Dynamixel Pro protocol.

III-E Software Design

The software can be broken down into two sections: software used on the PC and the firmware used on board the manipulator. A system block diagram of different software interaction can be seen in Fig. 5. Robot Operating System (ROS) [12] was used to handle the high level functionality of the system. Desired end effector poses and robot states were published using the ROS MoveIt! package [13]. This was published as a ROS JointState message type which was processed by the Teensy.

The low level firmware functions send commands to both the ClearPath and Dynamixel Pro motors and also

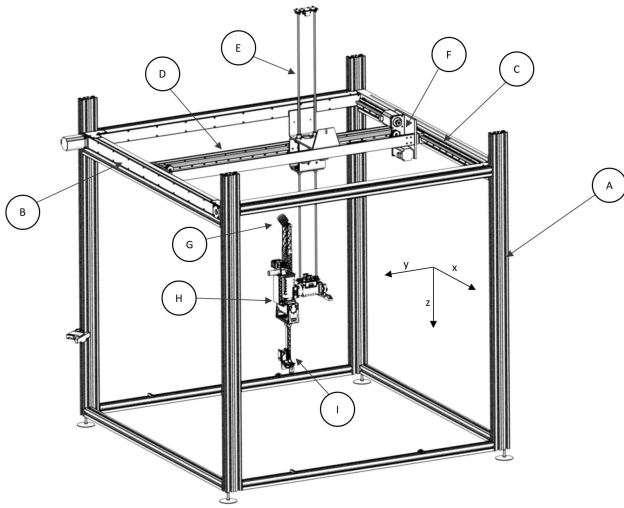


Fig. 4. Isometric view of the entire manipulator. Key components have been labelled and are as follows: (A) Aluminium T-slot stand, (B) Manipulator Aluminium frame, (C) X-Axis TBR20 profile rails, (D) Y-Axis TBR15 profile rails, (E) Z-Axis 10mm round rails, (F) Y-Z motor-carriage, (G) Suction gripper, (H) Wrist, (I) Parallel plate gripper

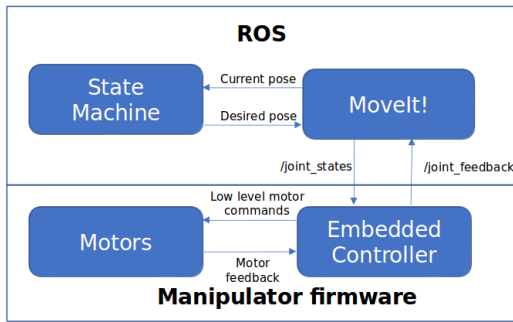


Fig. 5. System block diagram of the communication between software and firmware packages of the manipulator system.

read any feedback that was available from the motors. As the ClearPath motors are a drop-in replacement for regular stepper motors, a stepper motor library was able to be used. The library which was used is AccelStepper [14], a library for use with Arduino compatible devices. This expands on the standard Stepper library provided by Arduino. The main benefit in using AccelStepper is that it allows the user to control the acceleration profile of the motor which is desirable for this application. The Dynamixel Pro were controlled using a modified version of their OpenCR library [15]. The public open source library was developed to be used with their own electronic hardware. Slight modifications were made in order to adapt the library for use with the Teensy 3.6.

IV. PERFORMANCE EVALUATION

IV-A Methodology

In order to test whether the design specs have been met, the motion of the system was tested. OptiTrack Motive, a motion capture system was used to track trajectories during

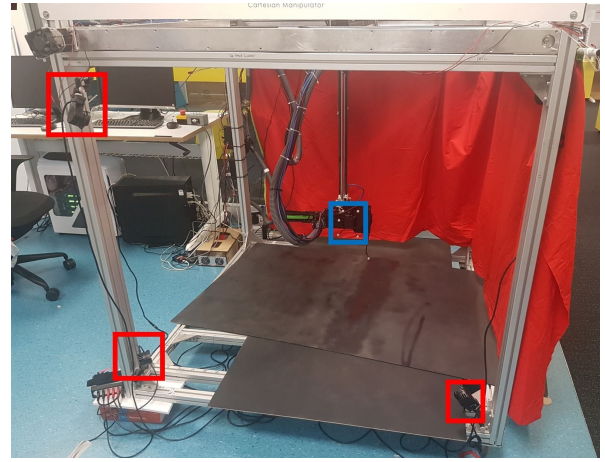


Fig. 6. Motion capture setup. Five motion capture cameras (red boxes) were used to determine the pose of the multi-reflective body (blue box)

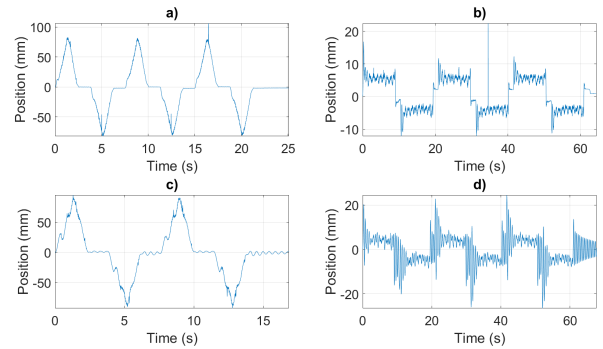


Fig. 7. Error in position of the X-axis. The X-axis is driven at fast and slow speed at a high and low Z-height. (a) high-fast, (b) high-slow, (c) low-fast, (d) low-slow.

different path executions. The setup can be seen in Fig. 6. Each axis was tested individually at various heights and speeds to test the end point accuracy during motion. Each axis was commanded at a fast and slow speed moving to and from the extremes of the tracking system. The pose of the multi-reflective body seen in Fig. 6 is tracked and interpolated to compare the desired joint position with recorded position whilst in motion and for steady state error.

IV-B Results

A summary of the tests conducted can be found in Table I. Below are the plots of that data that was captured and summarised in these tables.

X-axis: The results of X-axis movements can be seen in Fig. 7. The steady can be seen to converge to close to zero once motion has ceased. The average error in position is 9.62 mm as seen in Table I. During slow movements, oscillations occur about the desired point due to the pendulum effect but still converge to the desired end point. This is considered sufficient for the application that the manipulator is designed for.

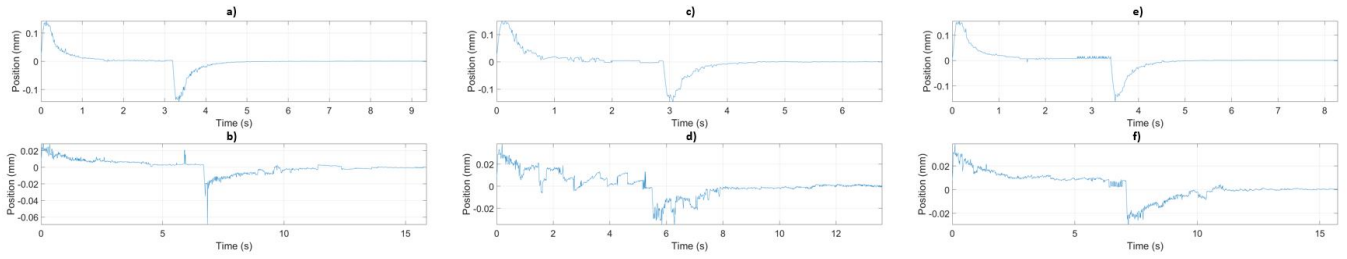


Fig. 8. Wrist trajectory at fast and slow speeds. (a) roll-fast, (b) roll-slow, (c) pitch-fast, (d) pitch-slow, (e) yaw-fast, (f) yaw-slow.

TABLE I
SUMMARY OF ERROR ACROSS SINGLE AND MULTIPLE AXES

	Standard Deviation	Mean Error	Static Error
x	16.07	9.62	$6.2e^{-01}$ mm
y	13.73	9.42	$1.9e^{-01}$ mm
z	13.70	7.91	$1.9e^{-03}$ mm
xzy	64.88	29.63	$1.5e^{-01}$ mm
roll	0.02	0.01	$5.6e^{-04}$ rad
pitch	0.02	0.01	$1.5e^{-04}$ rad
yaw	0.02	0.01	$7.3e^{-05}$ rad

Each axis is driven individually and simultaneous motion of axes are also evaluated (xyz). Mean error is defined as the error between the desired position and the measured position. Static error is the error between desired position and measured position once motion has ceased.

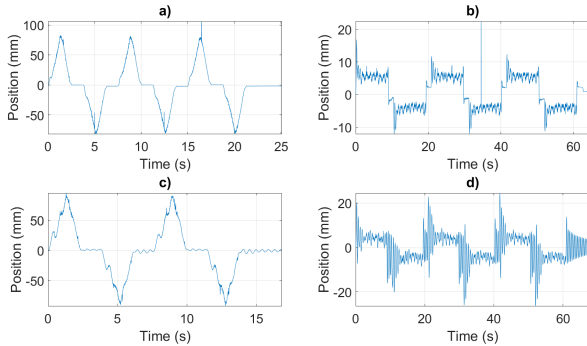


Fig. 9. Error in position of the Y-axis. The Y-axis is driven at fast and slow speed at a high and low Z-height. (a) high-fast, (b) high-slow, (c) low-fast, (d) low-slow.

Y-axis: As seen in Fig. 9, the Y-axis trajectory oscillates substantially at low heights at slow speeds. This is caused by the pendulum effect of the system as described in Section III. For the task of the Amazon Robotics Challenge, final point accuracy is more crucial than in-motion accuracy. We can see that the final desired position converges to almost zero. Given this specific task, slow Y-axis movements are not necessary any way.

The coupling effect of the differential belt system is also of interest. The trajectory of the Z-axis while moving the Y-axis can be seen in Fig. 10. We can see that the Z-axis shows a small translation during pure Y-axis motion as a result of the differential belt system. This is to be expected as the two ClearPath motors would need to be perfectly synchronised in order to reduce this movement to zero. Despite this travel, the final point accuracy results in no

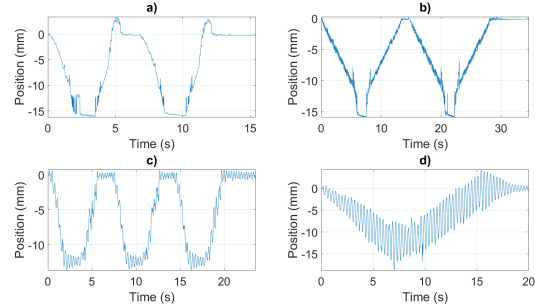


Fig. 10. Z-axis trajectory during pure Y-axis motion. The oscillations are a result of the pendulum effect. (a) high-fast, (b) high-slow, (c) low-fast, (d) low-slow.

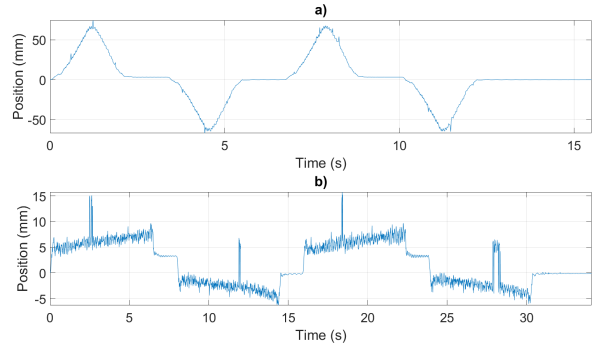


Fig. 11. Z-axis trajectory at various speeds. (a) high-fast, (b) high-slow, (c) low-fast, (d) low-slow.

unwanted Z-axis translation.

Z-axis: The Z-axis can follow a pure Z trajectory with a fair amount of accuracy as seen in Fig. 11. The Z-axis exhibits the least amount of error while in motion with only 7.9 mm mean error in position. As discussed previously, due to the coupling of the Y- and Z-axes, the Y-axis wanders during pure Z-axis motion just as the Z-axis wanders during pure Y-axis motion. Despite this, steady state precision is still achieved.

Wrist - roll, pitch and yaw: The wrist joint of the robot exhibit exceptional accuracy not only in motion but in steady state as well as seen in Fig. 8. Achieving a steady state of almost zero error.

XYZ axes: Simultaneous motion of multiple axes were tested against a more complex trajectory. A lemniscate curve was generated on firstly a single plane at three different heights and also in a multi-plane test. The system was tested

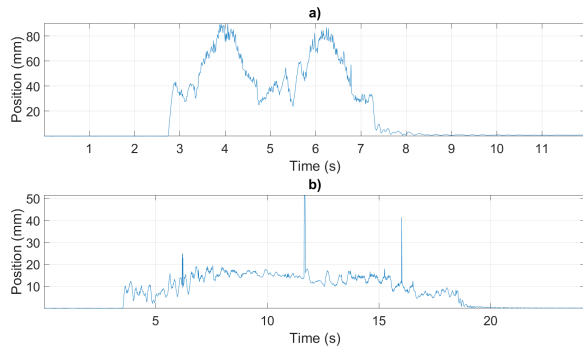


Fig. 12. Three axis movements in the X-, Y-, and Z-axes. (a) xyz-fast, (b) xyz-slow.

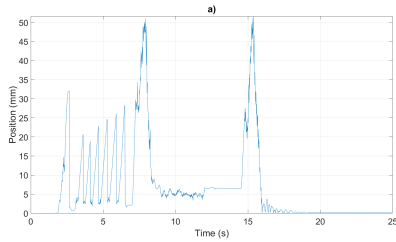


Fig. 13. Example trajectory of a real pick. The task was to pick up a 1kg dumbbell from a start point, place it in another area and return to the start position

at different speeds and exhibited the same characteristics as the single axis. Steady state error is almost zero seen in Fig. 12.

Example Pick run: To simulate a pick task within the Amazon Robotics Challenge a simple scenario was set up in order to test accuracy during motion the manipulator was intended for. The task was to pick an item from the Amazon item set, in this case a 2lb weight, and place it to another location and then return to its start position. The trajectory recorded can be seen in Fig. 13. The manipulator was easily able to achieve the task with a mean error of only 2.96mm during motion.

IV-C Verification

Using the data presented in this section, we can verify our speed specifications. Unfortunately due to mechanical limitations, the system experienced belt slip under high accelerations. As a result the acceleration parameter of the controller needed to be lowered. Table II provides a summary of the speed and error achieved by each axis. We've shown that the system is capable of moving a load whilst following linear trajectories with reasonable accuracy. Table I features the static error for each axis. We found that despite oscillations and trajectory error during motion, the steady state error is negligible and can achieve sub-mm and sub-mrad accuracy.

V. DISCUSSION AND CONCLUSION

As seen in section IV-B we've shown the limitations of the system in terms of trajectory motion. Y-axis motion contributes the most to the overall error due to the pendulum effect of the system. We've shown that this only happens

TABLE II
SUMMARY OF SPEEDS ACHIEVED BY THE SYSTEM

Axis	Commanded Speed	Achieved Speed	% Error
x	0.604	0.572	5%
y	0.531	0.493	7%
z	0.512	0.472	8%
roll	1.547	1.687	-9%
pitch	1.536	1.531	0%
yaw fast	1.593	1.660	-4%

As the controller used for the system is a position controller, negative error values indicate that the joint is able to track cope with latency and accurately track a trajectory.

at low speeds at approximately speeds of 0.1m/s or less. Forcing fast movements can avoid this behaviour but may possibly limit the applications of which this design can be used. Additionally, the pendulum effect can be minimised by retracting the Z-axis when performing large translations. The maximum target speed was not able to be reliably achieved due to belt slippage. As a result, the acceleration of the system was limited yielding a maximum achieved speed of only 0.57 m/s. In future we wish to address this issue as well as the slow movement oscillations by increasing the stiffness of the Z-axis rail and bearing system.

REFERENCES

- [1] L. Sciavicco and B. Siciliano, *Modelling and control of robot manipulators*. Springer Science & Business Media, 2012.
- [2] A. H. Qureshi, K. F. Iqbal, S. M. Qamar, F. Islam, Y. Ayaz, and N. Muhammad, "Potential guided directional-RRT* for accelerated motion planning in cluttered environments," in *IEEE International Conference on Mechatronics and Automation*. IEEE, Aug 2013, pp. 519–524.
- [3] D. Morrison, A. W. Tow, *et al.*, "Cartman: The low-cost cartesian manipulator that won the amazon robotics challenge," in *IEEE International Conference on Robotics and Automation (ICRA)*, 2018.
- [4] Amazon Robotics, "AR Challenge :: Amazon Robotics," 2017. [Online]. Available: <https://www.amazonrobotics.com/#/roboticschallenge/rules>
- [5] N. Correll, K. E. Bekris, D. Berenson, O. Brock, A. Causo, K. Hauser, K. Okada, A. Rodriguez, J. M. Romano, and P. R. Wurman, "Analysis and observations from the first amazon picking challenge," *IEEE Transactions on Automation Science and Engineering*, 2016.
- [6] P. I. Corke, *Robotics, vision and control: fundamental algorithms in MATLAB*. Berlin, Heidelberg: Springer, 2011.
- [7] C. Lehnert, A. English, C. Mccool, A. W. Tow, and T. Perez, "Autonomous Sweet Pepper Harvesting for Protected Cropping Systems," *IEEE Robotics and Automation Letters*, vol. 2, no. 2, pp. 872–879, 2017.
- [8] C. Innocenti and V. Parenti-Castelli, "Singularity-free evolution from one configuration to another in serial and fully-parallel manipulators," *Journal of Mechanical Design*, vol. 120, no. 1, pp. 73–79, mar 1998.
- [9] K. Hauser and Kris, "Continuous Pseudoinversion of a Multivariate Function: Application to Global Redundancy Resolution," *Workshop on the Algorithmic Foundations of Robotics*, Jan 2017.
- [10] Y. Nakamura and H. Hanafusa, "Inverse Kinematic Solutions With Singularity Robustness for Robot Manipulator Control," *Journal of Dynamic Systems, Measurement, and Control*, vol. 108, 1986.
- [11] S. Wade-McCue, N. Kelly-Boxall, M. McTaggart, *et al.*, "Design of a Multi-Modal End-Effector and Grasping System: How integrated design helped win the Amazon Robotics Challenge," Australian Centre for Robotic Vision, Tech. Rep. ACRV-TR-2017-03, arXiv:1710.01439, 2017.
- [12] M. Quigley, B. Gerkey, K. Conley, J. Faust, T. Foote, J. Leibs, E. Berger, R. Wheeler, and A. Ng, "ROS: an open-source Robot Operating System," in *Proc. of the IEEE Intl. Conf. on Robotics and*

Automation (ICRA) Workshop on Open Source Robotics, Kobe, Japan, May 2009.

- [13] I. A. Sutan and S. Chitta, "MoveIt!" [Online]. Available: <http://moveit.ros.org/>
- [14] M. McCauley, "AccelStepper: AccelStepper library for Arduino," 2010. [Online]. Available: <http://www.airspayce.com/mikem/arduino/AccelStepper/>
- [15] R. L. W. Jung, "Robotis OpenCR." [Online]. Available: https://github.com/ROBOTIS-GIT/OpenCR/tree/master/arduino/opencr_arduino/opencr/libraries/DynamixelSDK